Supplementary Information

Dynamic one-dimensional water in a nonporous organic solid with optics response

Yong-Tao Wang,*[a] Gui-Mei Tang,*[a] Jin-Hua Wang,[a] Wen-Zhu Wan,[a] Tin-Xiao Qin,[a] Yong-Qiang Wang,[a] Kai-Li Mou,[a] Tian-Duo Li,[a] and Lu-Fang Ma*[b]

[a] Department of Chemical Engineering, Shandong Provincial Key Laboratory of Fine Chemicals, Qilu University of Technology, Jinan, 250353, P. R. China

[b] College Chemistry & Chemical Engineering, Luoyang Normal University, Luoyang, 471022, P. R. China.

* Corresponding author. E-mail: ceswyt@sohu.com Fax: +086 0531 8900 0551; Tel: +086 0531 8900 0551;

Content

Experiment Section

Materials and instruments: The reagents and solvents employed were commercially available and used as received without further purification. Elemental analyses were performed on a Perkin-Elmer 240 elemental analyzer. The FT-IR spectra were recorded from KBr pellets in range 400-4000 cm^{-1} on a Bruker Tensor27 spectrometer. The chamber was filled with the dried flowing nitrogen gas. Fluorescence spectra were taken using Varian Eclipse fluorescence spectrophotometer. To in order to the intensity value, the wooden solid sample holder acting as the internal reference was applied during the process of measuring the luminescent spectra. Thermal analyses were performed on a SDT Q600 instrument in N_2 atmosphere with a heating rate of 10^{o}C/min from room temperature to 450 ^{o}C. Powder X-ray diffraction (PXRD) data were obtained by using a Bruker D8 ADVANCE diffractometer with Cu Ka (λ =1.54056 Å) radiation at an RH of 30% at ambient temperature. A step size of 0.03^{o} and counting time of 0.1s/step were applied in a 2θ range of 5.00-60.00 degree. Kurtz powder SHG measurements were performed on ground samples of crystalline **L·2H$_2$O** (**1**) and **L·3H$_2$O** (**2**) with a synchroscan streak camera (Hamamatsu Model C1587, 8 ps resolution) connected to a polychromator as the detector system, and an optical parametric generator (Spectra Physics, Model: OPA-800C) pumped by a mode-locked Ti: sapphire laser oscillator–amplifier system (Spectra Physics, Model: Hurricane) as the pump source. The powder second-harmonic signals were compared to that of KH_2PO_4 (KDP) to determine the relative SHG efficiencies of **1** and **2**.

Measurement of the time-dependent spectral of apohost L upon exposure to water vapor: The guest-free crystal of host **L** was placed in a chamber saturated with water vapor at 100 °C. The exposed sample was taken out at different time intervals, and the measurement of the PXRD, IR, and fluorescence spectra was carried out.

Thermogravimetric analyses (TGA) in 1 and 2: To determine the thermal stability of 1D chain/tape in **1** and **2**, their TGA behaviors were measured. The TGA figure in compound **1** show that the weight loss of 17.82 % occurred at the temperature arrange of 30-110 ^{o}C (Fig. S7a), which is slightly higher than the calculated value (15.38 %). For **2**, the weight loss assigned to the gradual release of three water molecules per formula unit is observed in the range 35-112 ^{o}C (obsd, 21.08%; calcd, 21.43%) (Fig. S7b).

X-ray Crystallography. Single-crystal X-ray diffraction data for compounds **L, 1 and 2** were collected on a Bruker CCD APEX diffractometer at room temperature with Mo Kα radiation (λ = 0.71073 Å). All the structures were solved by direct methods using the SHELXS program of the SHELXTL package and refined by full-matrix least squares methods with SHELXL.[1] All non-hydrogen atoms were located in successive difference Fourier syntheses, where they were refined with anisotropic thermal parameters on F^2. Hydrogen atoms bonded to carbon atoms were located at geometrically calculated positions; the aqua hydrogen atoms are located from difference maps, which were refined with isotropic thermal parameters. The data of the weak interactions were calculated by PLATON.[2] Crystallographic data and structural refinements for compounds **L, 1** and **2** are summarized in Table S1.

CCDC reference number 734294, 734295, and 734296 for **L**, **1**, and **2**, respectively. These data can be obtained free of charge via www.ccdc.cam.ac.uk/conts/retrieving.html (or from the Cambridge Crystallographic Data Centre, 12 Union Road, Cambridge CB21EZ, UK; fax: (+44) 1223-336-033; or deposit@ccdc.cam.ac.uk).

Synthesis of 2-(1*H*-imidazol-1-ylmethyl)-1*H*-benzimidazole (L), 1, and 2

Method A for preparing anhydrous L, 1 and 2:

2-(1*H*-imidazol-1-ylmethyl)-1*H*-benzimidazole (L). The **L** was prepared by the literature.[3] The **L** (0.5 g) was solved in the hot water (3 mL). After two day, the pale-yellow block crystals suitable to X-ray single diffraction were obtained. The IR spectra, EA and NMR of **L** were accordance with those of the reported value.[3]

L·2H$_2$O (1). The **L** (0.2 g) was exposed to the water vapor at 100 °C. After about 1 day, the pale-yellow block crystals (**1**) suitable to X-ray single diffraction were obtained. Yield: 0.192 g (81.25%). IR (KBr, cm^{-1}): 3425(v-br), 3147(m), 1605(m), 1519(s), 1470(m), 1422(m), 1333(m), 1316(m), 1300(s), 1243(m), 1196(w), 1112(m), 1083(m), 1061(w), 1027(m), 999(m), 942(w), 882(w), 863(m), 823(m), 772(w), 755(m), 729(m), 661(w), 644(m), 617(m), 497(w), 439(m); Elemental analysis calcd (%) for $C_{11}H_{14}N_4O_2$ (234.26): C, 56.40; H, 6.02; N, 23.92; found: C, 56.73; H, 6.05; N, 23.81.

L·3H$_2$O (2). The **L** (0.2 g) was exposed to the water vapor at 100 °C. After about 1.5 days, the pale-yellow block crystals (**2**) suitable to X-ray diffraction were obtained. Yield: 0.211 g (82.91%); IR (KBr, cm^{-1}): 3425(v-br), 3124(m), 3052(w), 3025(w), 1607(m), 1511(m), 1472(m), 1425(vs), 1377(m), 1340(w), 1297(w), 1281(s), 1205(w), 1190(m), 1148(w), 1114(m), 1080(m), 1056(w), 1026(w), 1001(w), 963(m), 918(m), 907(m), 889(w), 872(m), 844(m), 823(m), 769(m), 748(s), 663(m), 613(m), 444(m); Elemental analysis calcd (%) for $C_{11}H_{16}N_4O_3$ (252.28): C, 52.37; H, 6.39; N, 22.21; found: C, 52.85; H, 6.36; N, 22.29.

Method B for preparing anhydrous L, 1 and 2:

Crystals of **L**·3H$_2$O (**2**) were obtained by the slow evaporation of an aqueous solution of **L**. Crystals of **L**·2H$_2$O (**1**) and anhydrous **L** were obtained by gradual dehydration of **2**, respectively.

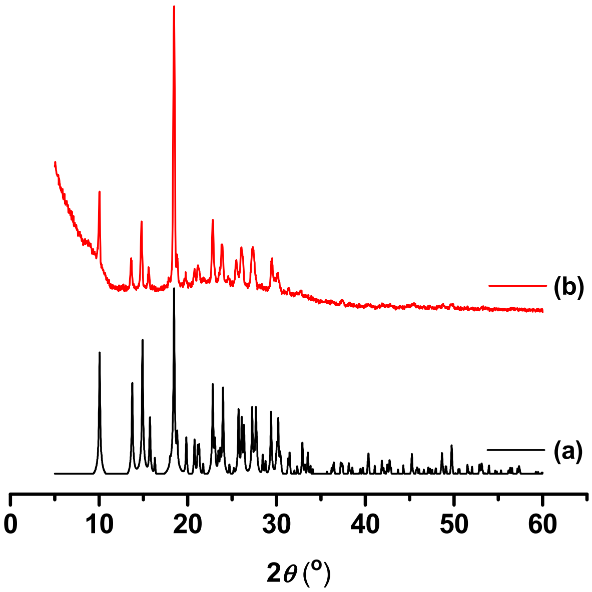

Fig. S1 Powder X-ray diffractometer (PXRD) patterns of compound **L**: (a) simulated; (b) powdered.

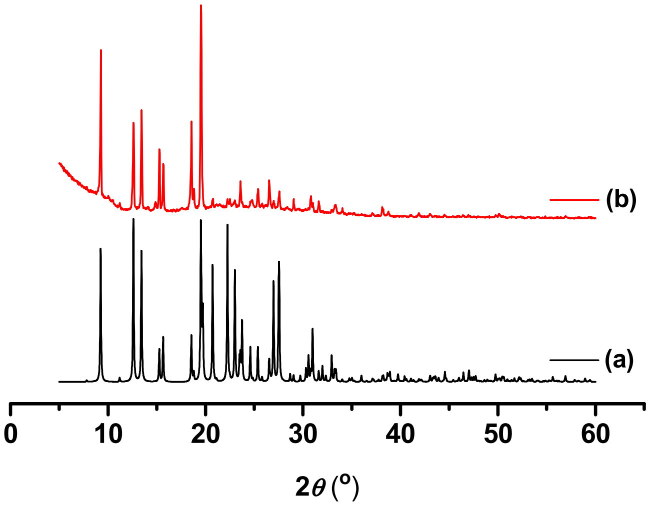

Fig. S2 PXRD patterns of compound **1**: (a) simulated; (b) powdered.

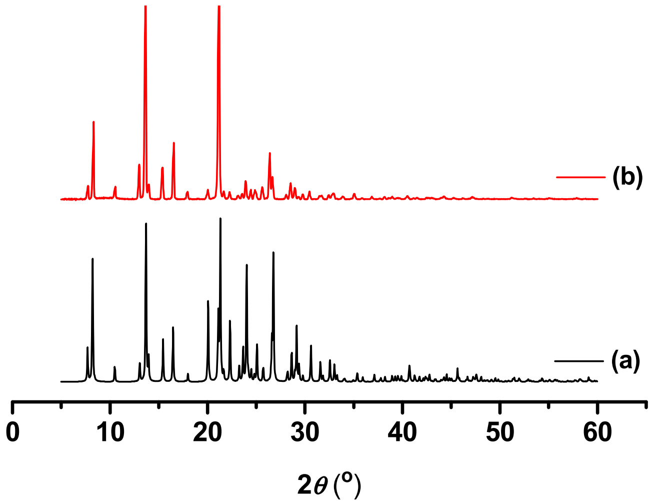

Fig. S3 PXRD patterns of compound **2**: (a) simulated; (b) powdered.

Table S1 Crystallographic data and structure refinements for **L, 1** and **2**

Compound reference	**L**	**1**	**2**
Chemical formula	$C_{11}H_{10}N_4$	$C_{11}H_{14}N_4O_2$	$C_{11}H_{16}N_4O_3$
Formula Mass	198.23	234.26	252.28
Crystal system	Monoclinic	Orthorhombic	Orthorhombic
a/Å	7.0582(13)	14.032(8)	13.554(2)
b/Å	17.577(3)	19.114(10)	21.511(3)
c/Å	8.5676(16)	4.625(3)	4.5170(7)
α/°	90.00	90.00	90.00
β/°	101.257(2)	90.00	90.00
γ/°	90.00	90.00	90.00
Unit cell volume/Å^3	1042.5(3)	1240.4(12)	1317.0(3)
Temperature/K	296(2)	296(2)	296(2)
Space group	$P2_1/n$	$Pna2_1$	$Pna2_1$
No. of formula units per unit cell, Z	4	4	4
Absorption coefficient, μ/mm^{-1}	0.081	0.090	0.095
No. of reflections measured	8798	10276	10153
No. of independent reflections	2408	2857	2667
R_{int}	0.0281	0.0518	0.0380
Final $R_1{}^a$values ($I > 2\sigma(I)$)	0.0537	0.0468	0.0383
Final $wR(F^2)^b$ values ($I > 2\sigma(I)$)	0.1209	0.1029	0.1034
Final $R_1{}^a$ values (all data)	0.0714	0.0983	0.0562
Final $wR(F^2)^b$ values (all data)	0.1299	0.1263	0.1179
Goodness of fit on F^2	1.198	1.006	0.831
Number of CCDC	734294	734295	734296

^{a} $R_1 = \sum||F_o|-|F_c||/\sum|F_o|$. ^{b} $wR_2 = [\sum[w(F_o^2-F_c^2)^2]/\sum[w(F_o^2)^2]]^{1/2}$.

Table S2 Hydrogen bond geometries in the crystal structures of **L**, **1** and **2**

Complex	D–H···A	H···A (Å)	D···A (Å)	D–H···A (°)
L[i]	N4–H4···N1[a]	1.92(3)	2.834(3)	178(2)
	C3–H3···N3[b]	2.60(2)	3.471(2)	152(2)
1[ii]	O1–H1A···N1[a]	1.93	2.754(4)	164
	O1–H1B···O2	2.01	2.838(4)	165(4)
	O2–H2A···O1[b]	1.86	2.702(4)	170(4)
	O2–H2B···N4[c]	1.91	2.758(3)	177
	N3–H3A···O2	1.90(3)	2.794(3)	179(3)
	C4–H4A···O1[d]	2.51(3)	3.502(4)	162(2)
2[iii]	O1W–H1WB···O2W	1.87(3)	2.716(2)	175(3)
	O1W–H1WA···O3W[a]	1.87(4)	2.705(3)	168(3)
	N3–H3···O1W[b]	2.02(3)	2.809(3)	174(2)
	O3W–H3WB···N4	1.96(3)	2.792(2)	166(3)
	O3W–H3WA···O1W	1.93(2)	2.783(3)	178(2)
	O2W–H2WB···O2W[c]	1.93(2)	2.776(3)	175(4)

O2W–H2WA···N1[d]	1.93(3)	2.761(3)	166(4)
C4–H4A···N4[a]	2.4900	3.333(3)	145(1)

Symmetry codes: [a]1 - x, -y, -z; [b]x, y, -1 + z for **L**[i]. [a]-x, 2 - y, -1/2 + z; [b]x, y, 1 + z; [c]1/2 + x, 3/2 - y, z; [d]x, y, 1 + z for **1**[ii]. [a]x,y, -1 + z; [b]-1/2 + x, 1/2-y, z; [c]2 - x, 1 - y, 1/2 + z; [d]2 - x, 1 - y, -1/2 + z for **2**[iii].

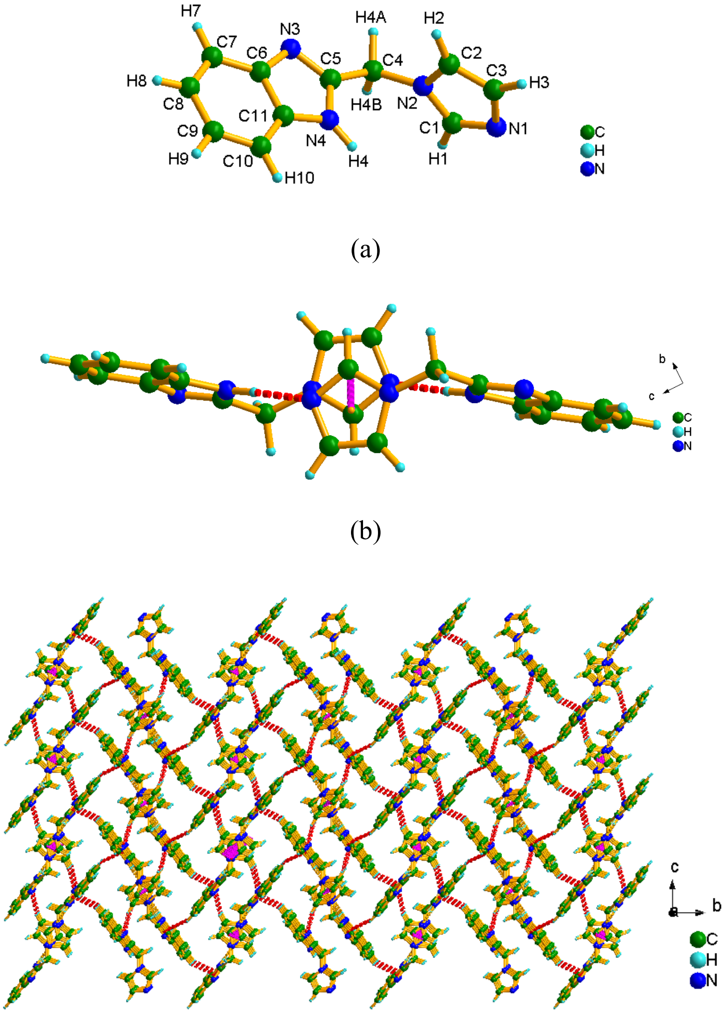

(a)

(b)

(c)

Fig. S4 (a) Ball-stick drawing of **L** in the asymmetric unit; (b) 1D tape of **L** along the *a* axis; (c) Packing diagram in **L** along the *a* axis. The purple dashed-lines represent hydrogen bonds and stacking interactions.

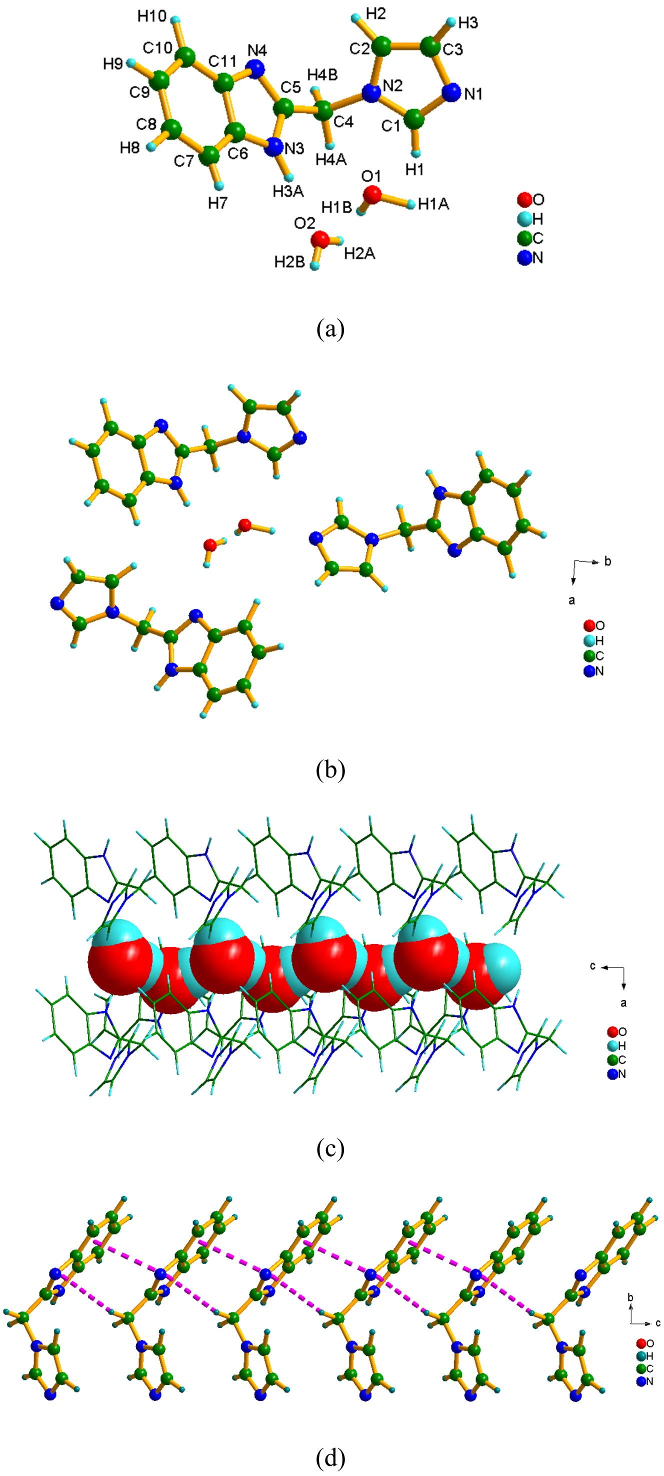

(a)

(b)

(c)

(d)

Fig. S5 (a) Ball-stick drawing of **1** in the asymmetric unit; (b) View point of 1D water chain extending along the *c* axis in **1**; (c) Closer view of 1D water chain in chain with space filling along the *b* axis. (d) Segment of packing diagram between **L** in **1** along the *a* axis. The purple dashed-lines represent C-H···π and π···π interactions.

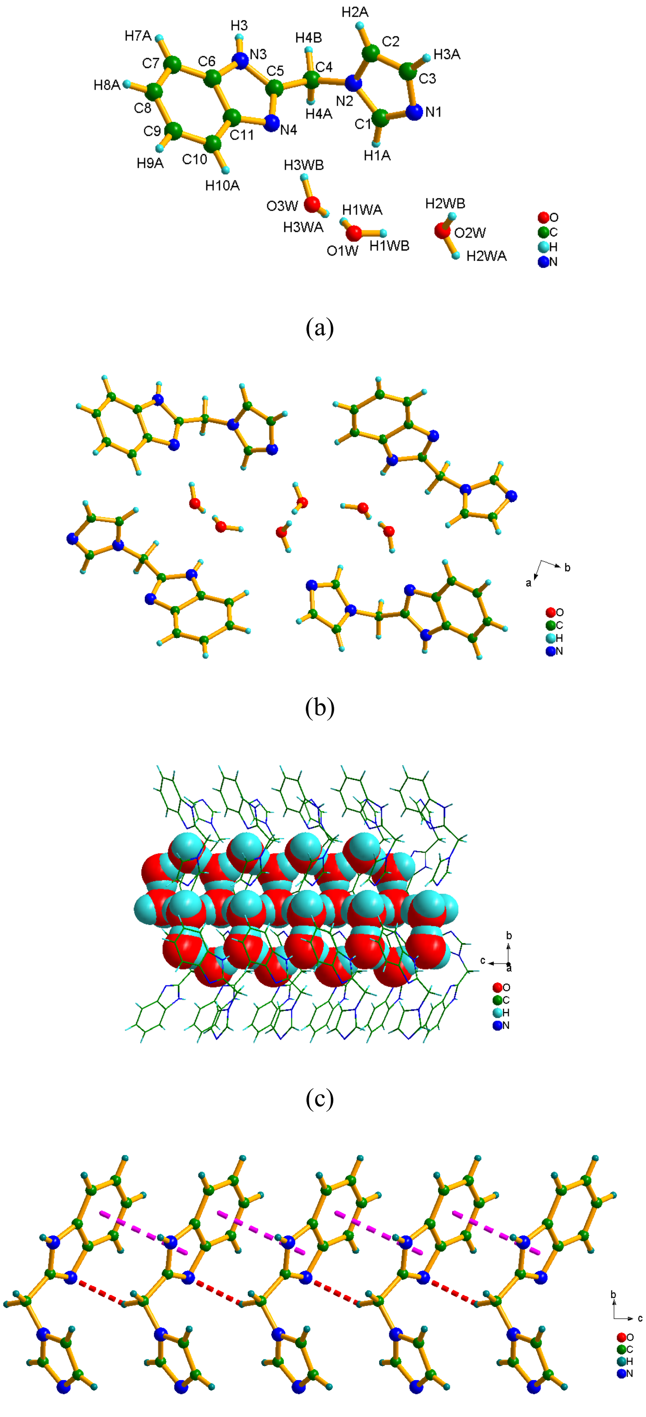

(a)

(b)

(c)

(d)

Fig. S6 (a) Ball-stick drawing of **2** in the asymmetric unit; (b) 1D water tape in **2** along the *c* axis; (c) Closer view of 1D water with space filling in **2**; (d) Segment of packing diagram of **2** along the *a* axis. The red dashed-lines and purple ones stand for hydrogen bonding and C-H···π packing interactions, respectively.

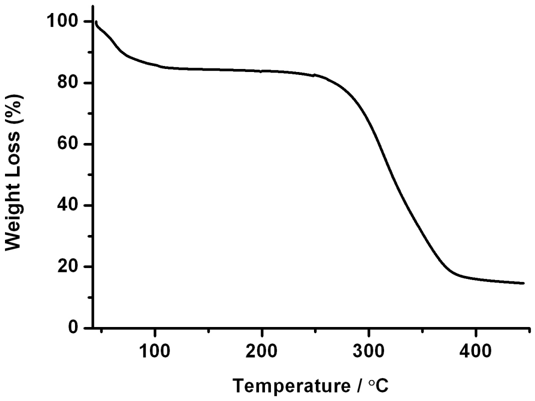

(a)

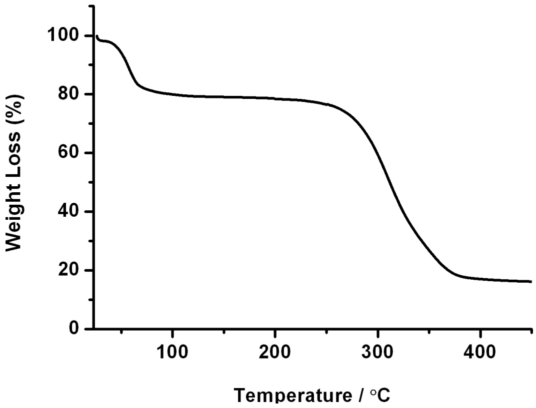

(b)

Fig. S7 TGA for **1** (a) and for **2** (b), respectively.

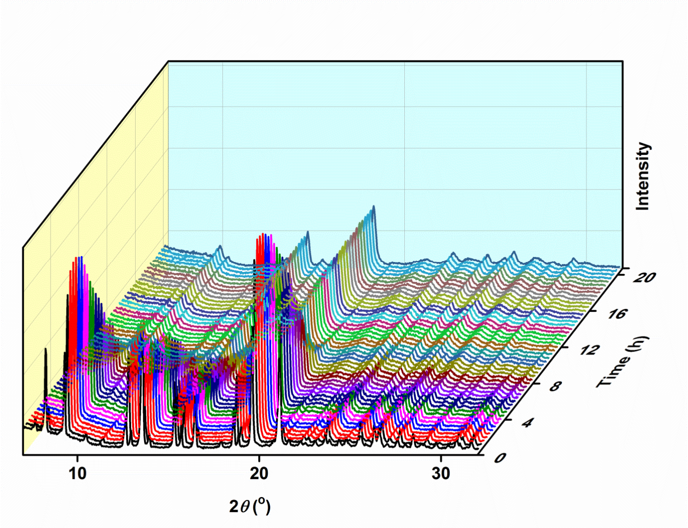

(a)

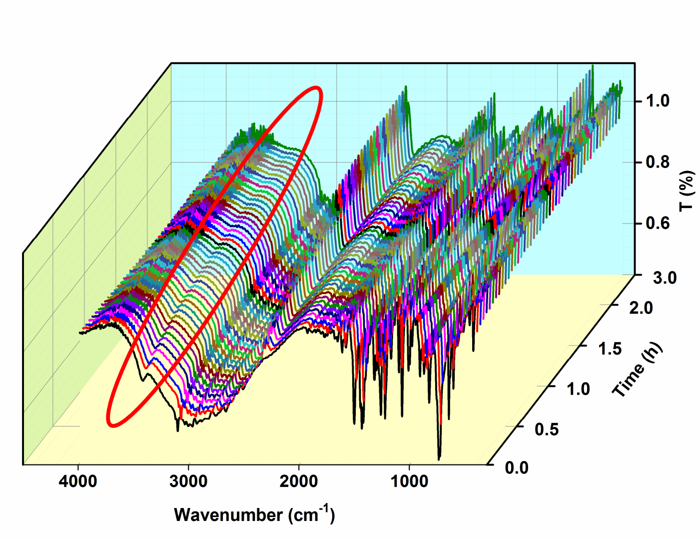

(b)

Fig. S8 (a) Time-dependent *in situ* PXRD in dehydration process from **2**, **1** to anhydrous **L** at ambient condition. (b) Time-dependent *in situ* IR spectra in dehydration process in the flow of dried N_2 at room temperature. The red circle represents the diminishing gradually of the water peaks upon the dehydration.

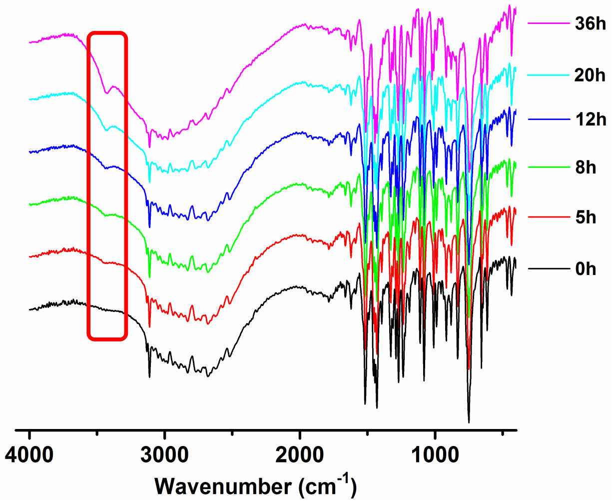

(a)

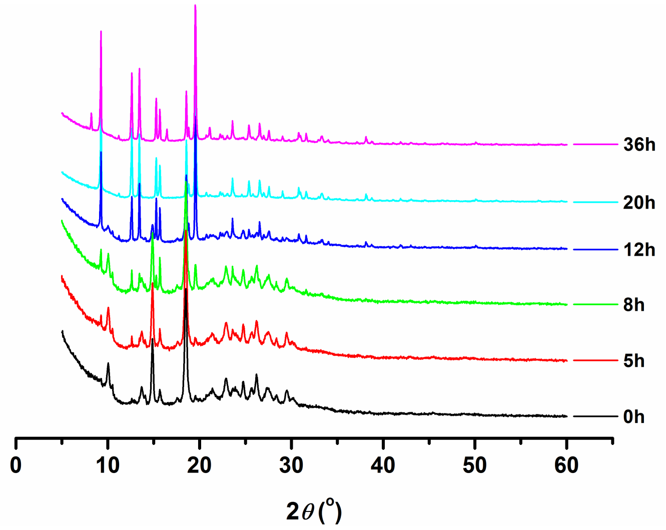

(b)

Fig. S9 (a) Time-dependent of IR spectra in rehydration process. (b) Time-dependent of PXRD in rehydration process. The rectangle circle represents the forming process for the peak of water upon the rehydration.

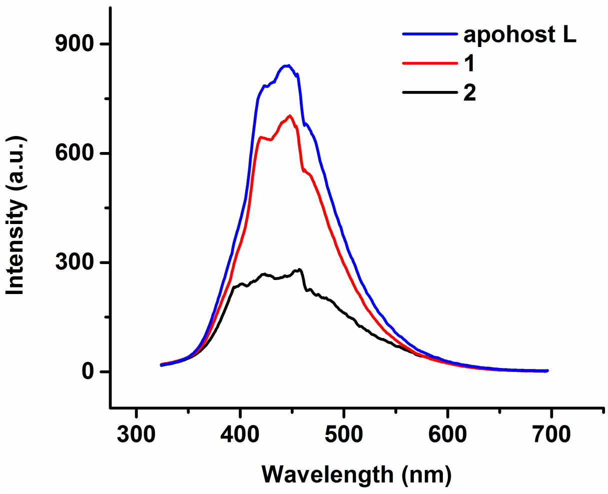

(a)

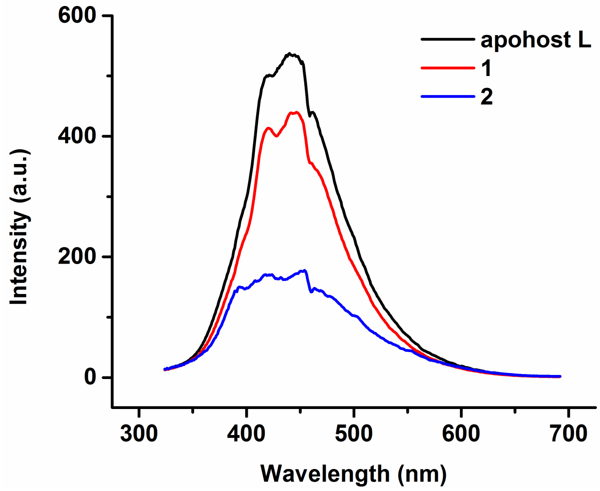

(b)

Fig. S10 (a) Solid state fluorescent spectra for apohost **L**, **1**, and **2** at room temperature, respectively. (b) Solid state fluorescent spectra for apohost **L**, **1**, and **2** at room temperature after rehydration, respectively.

Table S3 The supramolecular interactions in **L**, **1** and **2**.

Complex	Supramolecular interactions	Packing interactions (Å)
L	π (im)[a]···π (im)	3.637
	π (im)···π (im)	3.695
	C8-H8···π (phim)[b]	3.596
1	π (phim)···π (phim)	3.569(3)
	C4-H4B···π (phim)	3.437(4)
2	π (phim)···π (phim)	3.614

[a,b] The symbols im and phim stand for imidazole rings and benzoimidazole ones, respectively.

References

1 (a) G. M. Sheldrick, *SADABS*, University of Göttingen, Göttingen, Germany, 1996 and 2003; (b) G. M. Sheldrick, *SHELXTL NT Version 5.1. Program for Solution and Refinement of Crystal Structures*, University of Göttingen, Germany, 1997; (c) Bruker and AXS, *SAINT Software Reference Manual*, Madison, WI, 1998.

2 A. L. Spek, *Acta Crystallogr., Sect. A*, 1990, **46**, C34.

3 Y. T. Wang, G. M. Tang, Y. Q. Wei, T. X. Qin, T. D. Li, C. He, J. B. Ling, X. F. Long and S. W. Ng, *Cryst. Growth Des.*, 2010, **10**, 25.